General Disclaimer

One or more of the Following Statements may affect this Document

- This document has been reproduced from the best copy furnished by the organizational source. It is being released in the interest of making available as much information as possible.

- This document may contain data, which exceeds the sheet parameters. It was furnished in this condition by the organizational source and is the best copy available.

- This document may contain tone-on-tone or color graphs, charts and/or pictures, which have been reproduced in black and white.

- This document is paginated as submitted by the original source.

- Portions of this document are not fully legible due to the historical nature of some of the material. However, it is the best reproduction available from the original submission.

3

FINAL REPORT

E 7. 6 - 1 0.1 9.3

"A Cloud Physics Investigation
Utilizing Skylab Data"

Prepared for: Principal Investigator
Management Office
Code TF6
Johnson Space Center
Houston, Texas 77058

COTM: Zack H. Byrns

Prepared by: John Alishouse, Principal Investigator
National Oceanic and Atmospheric Administration
National Environmental Satellite Service
FOB #4
Washington, D. C. 20233

Co-Investigators: Dr. Herbert Jacobowitz
Dr. David Wark

EREP - 9611

Purchase Order No. T-4715B

Table of Contents

List of Figures

List of Tables

I. Introduction

The purpose of the Skylab Cloud Physics Investigation was to assess the feasibility of inferring certain cloud physical properties by remotely sensing reflected sunlight in selected spectral intervals. These properties are: cloud top pressure level, thermodynamic phase of the cloud particles, optical thickness, a particle size parameter, and the density of the particles. The spectral intervals originally proposed were in and just out of the oxygen A band at 763.0 and 754.0 nm respectively; in and just out of 2.0 μm CO_2 band at 2.06 and 2.12 μm respectively; and 1.61 μm. The particular functions of the channels are summarized in Table 1.

Table 1

Summary of Technique to Determine Cloud Physical Parameters

Parameter	Technique
Optical Thickness	Reflectance at 0.754 μm with theoretical relationship
Thermodynamic Phase	Reflectance ratio I (1.61)/I (2.125) as compared to theory
Particle Size	Reflectance ratio I (0.754)/I (2.125) as compared to theory
Cloud Top Altitude	Agreement in matching 0.763 μm altitude and 2.06 μm altitude with theory
Particle Density	Agreement in comparison of 0.763 μm and 2.06 μm altitude determination, optical thickness, and particle size data

II. Transmittance

Transmittance is a key parameter in determining cloud top pressure level. The carbon dioxide (2.0 μm) transmittance serves as a correction for cloud penetration for the oxygen transmittances.

A. Theoretical Results

1. O_2 Transmittance

Transmission calculations for the oxygen A band were performed in two different ways. Line-by-line calculations were performed using line parameters derived by Burch and Gryvnak [1]. The spectral bandwidth of the S191 radiometer in the A band region was such that the frequencies of interest overlapped into the .74 μm H_2O band. To investigate these effects, a copy of the Lowtran 2 [2] computer code was obtained.

Figures 1, 2, and 3 illustrate one of the problems associated with analyzing the S191 data, namely spectral resolution. The spectral resolution of the S191 in the A band region was about 20 nm. The term sec θ + sec φ is the sum of seconts of the solar zenith angle and radiometer nadir angle in the plane of the sun, satellite, and reflecting surface. A triangular instrument response function, $F=1-\left|\dfrac{\lambda - \lambda_o}{\Delta\lambda}\right|$, was assumed for these calculations.

Assume that we are trying to determine the pressure level of a cloud top. Assume that the cloud top is actually at 900 mb and that an error of 0.01 is made in the determination of the transmittance. For $\Delta\lambda$ = 20 nm and sec θ + sec φ = 2, this is an error of ±70 mb. For $\Delta\lambda$ = 5 nm the error is only ±30 mb. Figure 2 shows errors of a similar magnitude. Figure 3 shows the "reference" channel 754.0 nm for the spectral resolution of the S191. As can be noted the reference or out-of-band channel is now sufficiently wide that it overlaps into the oxygen absorption band on one side and a water vapor absorption band on the other.
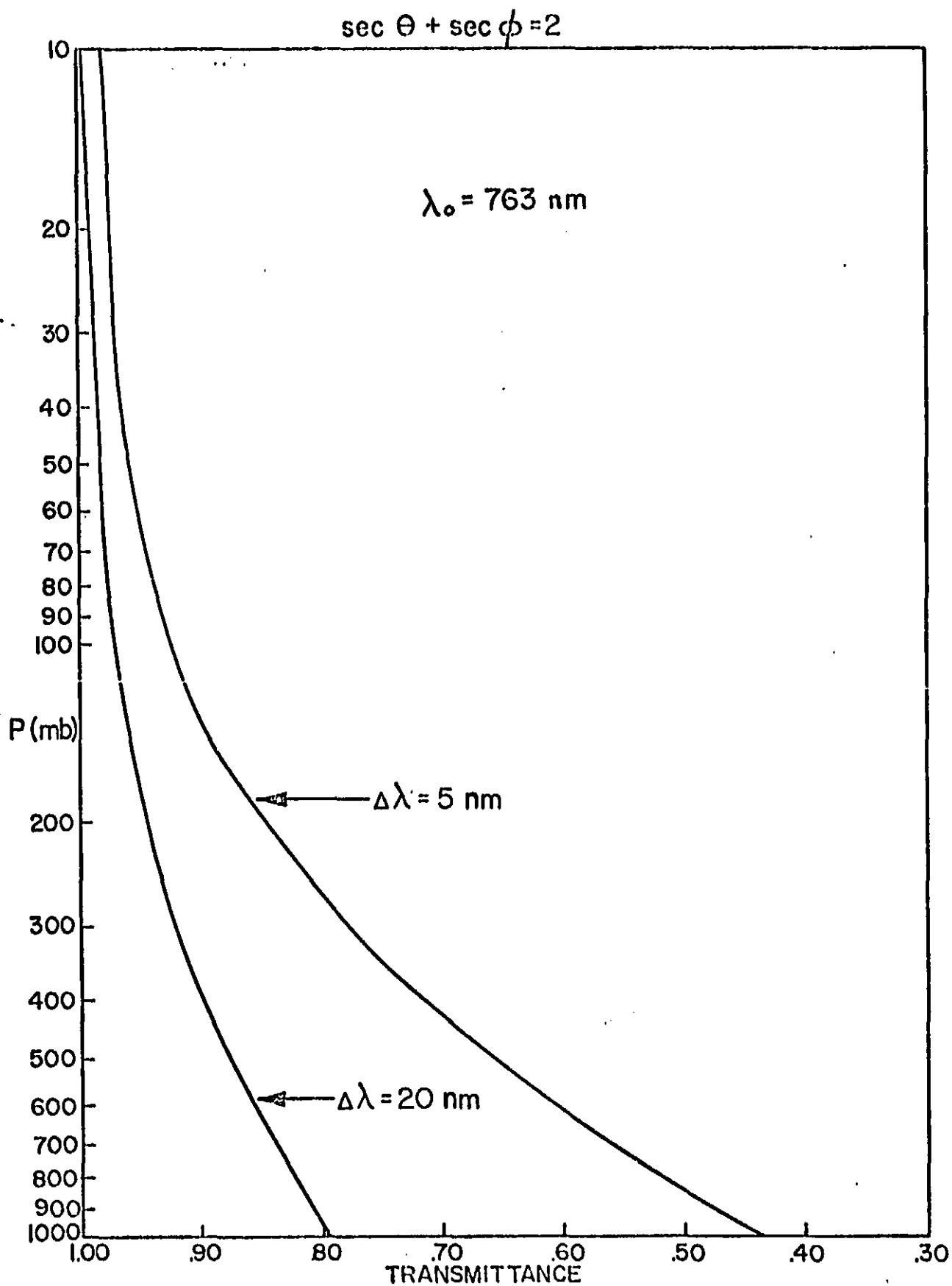
FIGURE 1   THIS FIGURE SHOWS TRANSMITTANCE AS FUNCTION OF PRESSURE FOR TWO FILTER HALFWIDTHS, 5 NM AND 20 NM.   20 NM IS THE RESOLUTION OF THE S-191.   SEC θ + SEC ϕ = 2 IS THE AIR MASS.

FIGURE 2   THIS FIGURE SHOWS TRANSMITTANCE AS A FUNCTION OF PRESSURE FOR THE SAME
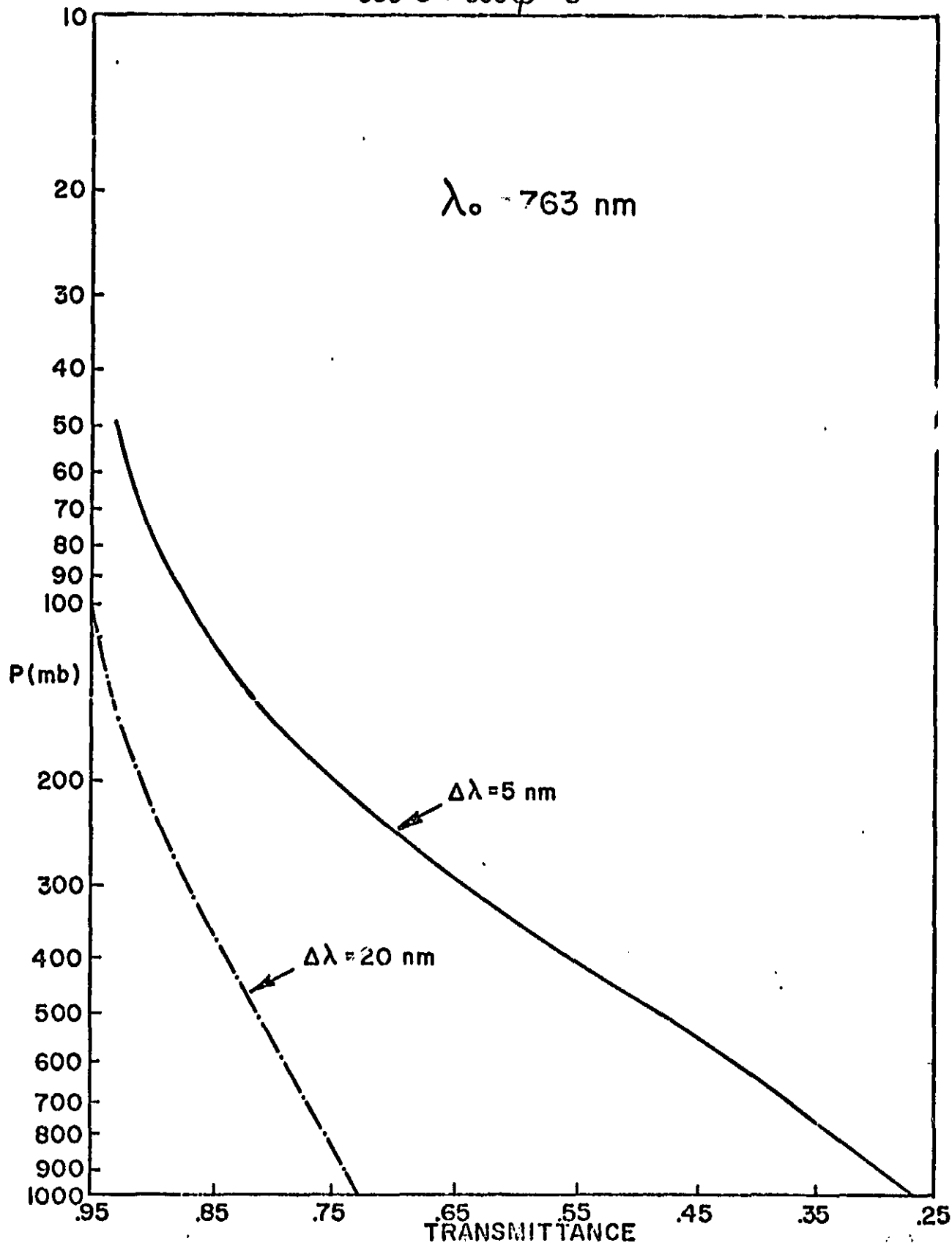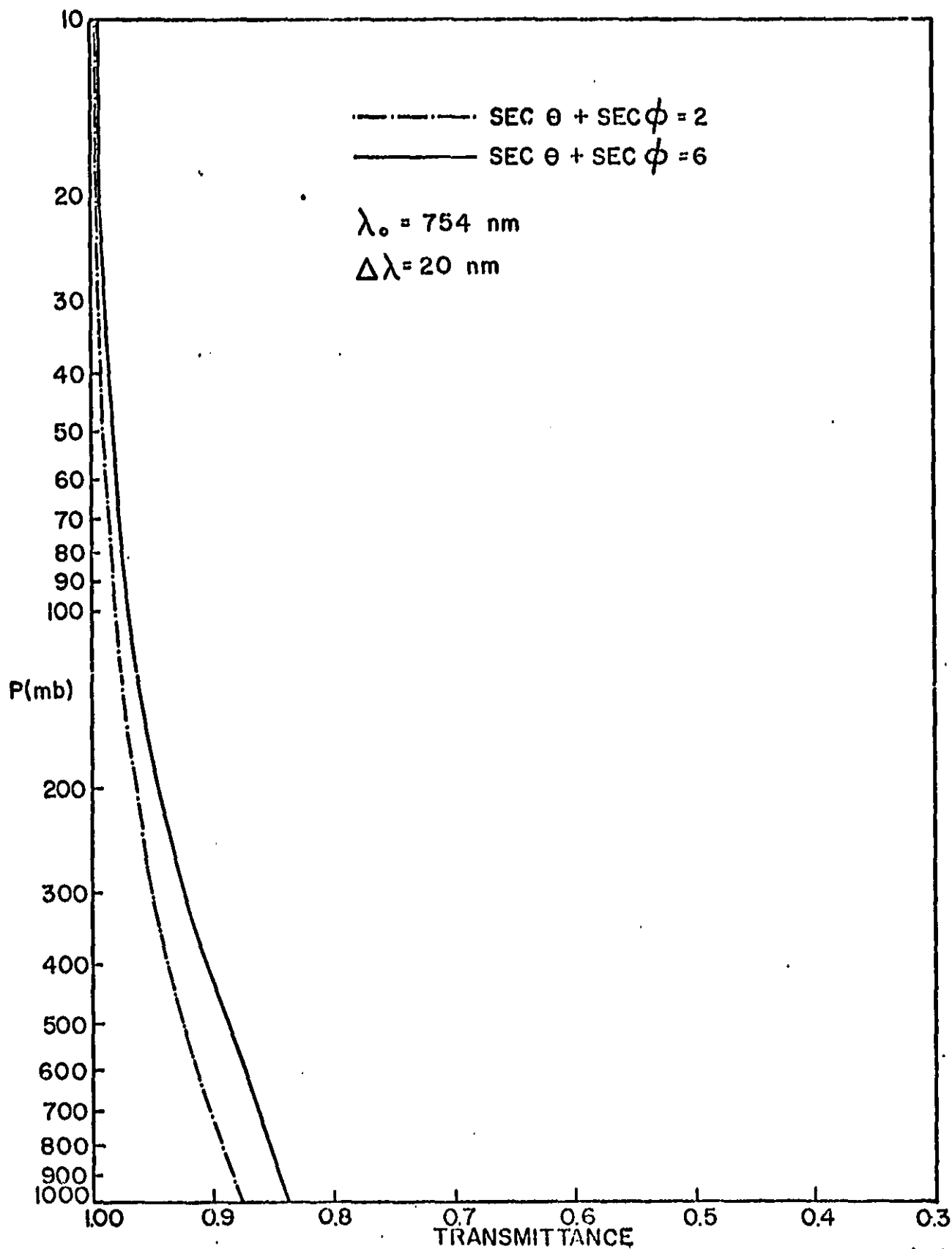TWO HALFWIDTHS AS FIG. 1, BUT FOR AN AIR MASS OF 6.

FIGURE 3   THIS FIGURE SHOWS TRANSMITTANCE AS A FUNCTION OF PRESSURE FOR THE REFERENCE WAVELENGTH, 754 NM.   THE SPECTRAL HALF-WIDTH IS 20 NM, THE RESOLUTION OF THE S-191.

In the S191 data for January 12, 1974, it was noted that the
intensity on the long wavelength side of the A band was greater
than that on the short wavelength side. This will be explained
in greater detail in the experimental results section. The Lowtran
2 program was used to investigate this effect as it contains
data for other atmospheric gases and aerosol models. Using a mid-latitude
winter model atmosphere with an aerosol distribution that corresponds to
a visibility of 23 km, transmittances were calculated between 833.3 nm
($12,000$ cm^{-1}) and 709.2 nm ($14,000$ cm^{-1}) in increments of 5 cm^{-1}. (The
Lowtran 2 program actually is parameterized in wavenumbers.) The triangular
instrument response function was used. The transmittances and instrument
response function were convolved with the solar irradiance spectrum [3] to
give irradiance values for solar zenith angles of $60°$ and $80°$ for heights of
0 and 5 km in the atmosphere. The results of these calculations are pre-
sented in Table 2. λ_1 is the wavelength of the relative maximum and the
short wave wavelength side of the A band and λ_2 is the relative maximum on
the long wavelength side of the A band. θ = solar zenith angle.

Table 2

h = 0 km

$\theta = 60°$ $\theta = 80°$

$\lambda_1 = 740.7$ nm, $\lambda_2 = 786.2$ $\lambda_1 = 741.8$ nm, $\lambda_2 = 788.0$ nm

$\dfrac{I(\lambda_1)}{I(\lambda_2)} = 1.040$ $\dfrac{I(\lambda_1)}{I(\lambda_2)} = .955$

h = 5 km

$\theta = 60°$ $\theta = 80°$

$\lambda_1 = 726.7$ nm, $\lambda_2 = 784.9$ nm $\lambda_1 = 727.0$ nm, $\lambda_2 = 786.5$ nm

$\dfrac{I(\lambda_1)}{I(\lambda_2)} = 1.100$ $\dfrac{I(\lambda_1)}{I(\lambda_2)} = 1.047$

$I(\lambda)$ is the computed irradiance at wavelength λ.

The most notable result of these calculations is the steadily decreasing irradiance ratio within increasing air mass. Finally ($h = 0$ km, $0 = 80^{\circ}$) the ratio becomes less than one, confirming the measurements. The other interesting feature is the shift to longer wavelengths of the relative maxima. A careful examination of the Lowtran results indicates that molecular (Rayleigh) scattering and aerosol scattering are about equally important in producing these shifts.

2.   2.0 µm CO_2 Band

In the spectral intervals of interest, 2.06 $\pm$.03 µm and 2.12 $\pm$.03 µm, there are about 3000 lines. While not all of these are strong enough to be considered in atmospheric absorption calculations, there are still too many lines to make line-by-line calculations practicable. Accordingly the Lowtran 2 [2] program was used together with an instrument response function and solar irradiance values [3] to compute the expected irradiances. The mid-latitude winter model atmosphere with an aerosol model corresponding to a visibility of 23 km was used. The transmission is defined as $\tau \equiv \dfrac{I(2.06 \text{ µm})}{I(2.12 \text{ µm})}$, where I is the computed atmospheric irradiance value. The results of these calculations are shown in Figure 4.

B.   Experimental Results

1.   General Information

The data to be analyzed were divided into categories by cloud type or snow. Measurements of sunlight reflected from snow fields
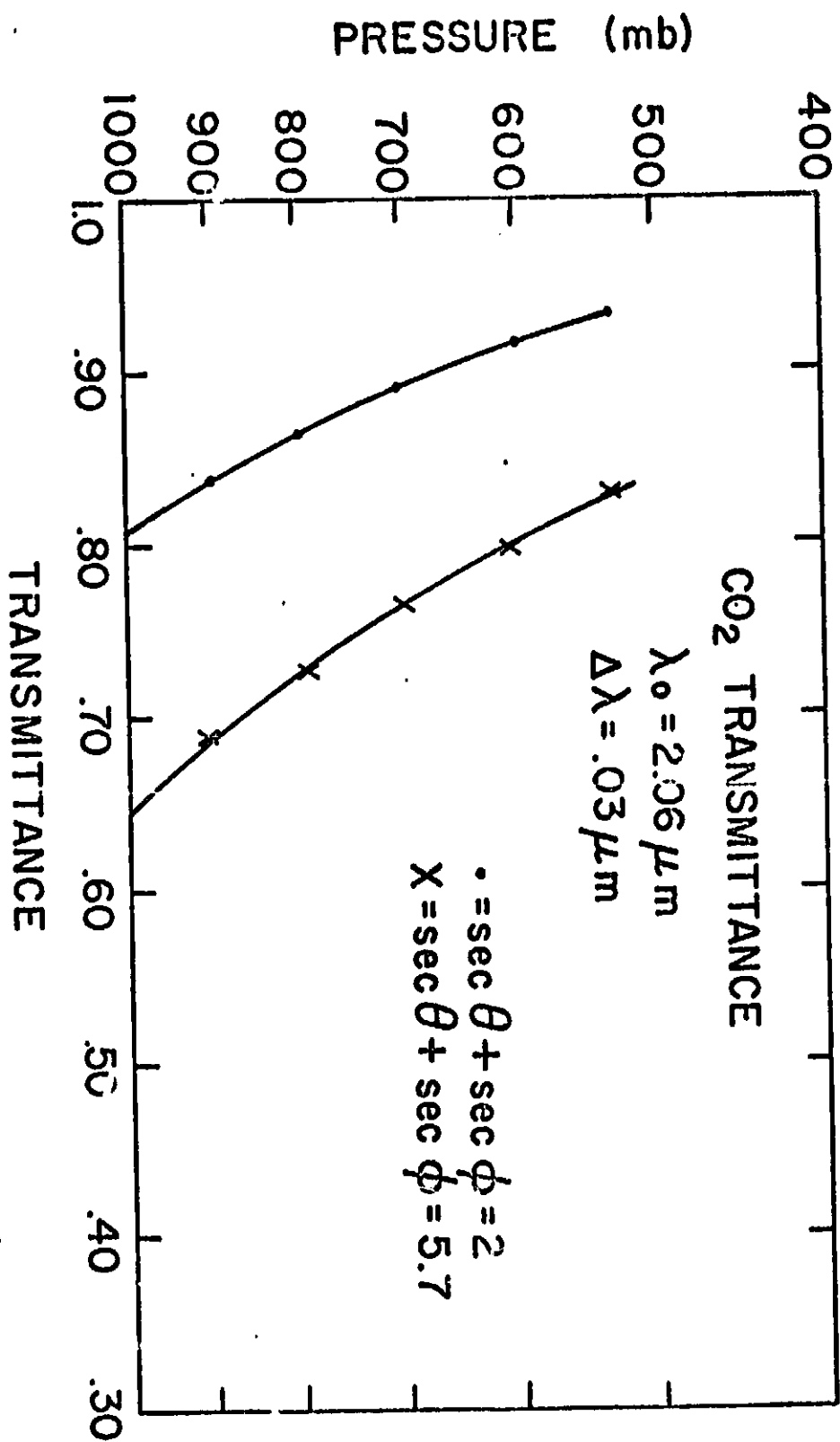
FIGURE 4 THIS FIGURE SHOWS TRANSMITTANCE AS A FUNCTION OF PRESSURE FOR 2.06 μM THE CO_2 ABSORPTION WAVELENGTH, THE SPECTRAL RESOLUTION, .03 μM, IS THAT OF THE S-191.

is particularly useful in that the pressure level (the earth's surface) of the reflecting surface is relatively easy to infer and there is no penetration problem. Thus the snow serves as a calibration point. Snow data were obtained for five days during the SL-4 mission, January 11, 12, 20, 22, and 24.

Another useful "calibration" target is the coastal stratus that occur frequently along the western United States. Their frequent occurrence, usually very uniform tops, and extent make them excellent targets. In addition they are almost certainly composed of liquid water droplets. Data for coastal stratus were obtained during the SL-3 mission on August 8, September 10, and September 15.

One of the goals of the experiment is to differentiate between water and ice clouds. It would therefore be desirable to obtain from clouds which are known to be uniquely one or other. Cirrus clouds are almost always composed of ice particles, so that spectra taken from cirrus would almost certainly be from clouds composed of ice particles. Data for cirrus were taken on June 5, December 1, December 2, and January 18.

Cloud layers of different heights are often associated with frontal systems. An unanswered question about this method of determining cloud physical parameters is how is it affected by multi-layer clouds. In the hope of answering this question and acquiring information about frontal clouds in general, spectra of frontal clouds were taken on June 4, June 12, June 13, August 5, August 9, January 25, and January 31.

Another cloud type of particular interest is the cumulonimbus or thunderstorm. Attempts were made to obtain spectra of Cb on June 4, June 13, August 5, and Spetember 12.

On June 9, and June 10, measurements were made of a tropical depression.

Due to the poor quality of the DAC imagery, the poor quality of the radiometric data, and the time constraints on the investigation, it was decided not to do further analysis on the SL-2 data.

2. A Band Results

Two methods of analysis for the A band data were considered and discarded as inadequate. Initially it was believed that sampling would be done frequently enough that the wavelengths of interest, .754 and .763 um could simply be read out and ratioed to give the transmissic . .pon examining the actual data it was found that the instrument was not sampled at these wavelengths or even the same wavelengths every time. Further it was noted that the wavelength of the absorption maximum (i.e., the band center) as determined by the JSC supplied wavelength calibration data was significantly different from its true position. An analysis of the calibration data revealed the two longer wavelength absorption bands in the BG-36 Schott glass and the band center of the A band formed nearly a straight line. A straight line was fit by least squares to these three points and this line was used as the wavelength calibration for the A band region. This is discussed more fully in Sec. IV.

Secondly it was intended to use a deconvolution procedure to improve the apparent spectral resolution of the data. However as the spectra often do not contain data at .754 and .763 μm the deconvolution procedure could not be used either.

3. CO_2 Band Results

The long wavelength data was processed in the following way: The raw data (counts) were converted to voltages and then to wavelength or radiance by algorithms recommended in $[7]$ or $[8]$ or described elsewhere in this report. The wavelengths of interest are 1.61 μm, 2.060 μm, and 2.125 μm. Screening criteria for wavelength were used to insure appropriate values were obtained. All wavelengths had to be within ±.003 μm of the specified wavelengths. The wavelength closest to the wavelength of interest was chosen and in the event of a tie (i.e., if samples were found at both +.001 μm and -.001 μm), then the long wavelength value would be chosen. The ratio of the radiance at 1.61 μm to the radiance at 2.125 μm was computed as was the ratio of the radiance of 2.06 μm to that at 2.125 μm. As each spectrum is identified by time, the program permitted averaging between two specified times. Mean values and standard deviations were computed for all radiances, wavelengths, and ratios. The data are presented by target type (i.e., snow, Ci, etc.), a particular day, and in some instances a particular day is subdivided into ranges of air mass.

Snow Data

January 11

$$\tau - \frac{(.06)}{I(2.125)} = .395 \pm .103 \qquad R = \frac{I(1.61)}{I(2.125)} = 3.553 \pm .423$$

The air mass ranged from 3.55 to 3.44

January 12

$$\tau = .354 \pm .068 \qquad R = 3.602 \pm .568$$

The air mass ranged from 3.57 to 3.39

January 20

$$\tau = .573 \pm .161 \qquad R = 3.045 \pm .451$$

The air mass ranged from 4.30 to 4.18

$$\tau = .527 \pm .127 \qquad R = ?.128 \pm .527$$

The air mass ranged from 4.16 to 4.11

January 22

$$\tau = .308 \pm .058 \qquad R = 3.320 \pm .285$$

The air mass ranged from 3.68 to 3.55

$$\tau = .324 \pm .045 \qquad R = 3.300 \pm .356$$

The air mass ranged from 3.55 to 3.39

$$\tau = .337 \pm .072 \qquad R = 3.378 \pm .281$$

The air mass ranged from 3.36 to 3.26

$$\tau = .349 \pm .078 \qquad R = 3.442 \pm .256$$

The air mass ranged from 3.25 to 3.24

January 24

$$\tau = .402 \pm .144 \qquad R = 3.336 \pm .747$$

The air mass ranged from 3.76 to 3.73

$$\tau = .428 \pm .150 \qquad R = 3.160 \pm .605$$

The air mass ranged from 3.73 to 3.72

$\tau = .352 \pm .060$ $\qquad\qquad$ $R = 3.657 \pm .379$

The air mass ranged from 3.52 to 3.40

$\tau = .378 \pm .086$ $\qquad\qquad$ $R = 3.566 \pm .426$

The air mass ranged from 3.36 to 3.23

Coastal Stratus Data

August 8

$\tau = .576 \pm .048$ $\qquad\qquad$ $R = 3.681 \pm .220$

The air mass ranged from 3.37 to 3.17

September 10

$\tau = .636 \pm .027$ $\qquad\qquad$ $R = 3.598 \pm .158$

No DAC data were taken during this pass, however the estimated range of the air mass was from 2.5 to 2.1.

September 15

$\tau = .668 \pm .026$ $\qquad\qquad$ $R = 2.805 \pm .128$

The air mass ranged from 2.66 to 2.45

$\tau = .655 \pm .034$ $\qquad\qquad$ $R = 3.142 \pm .201$

The air mass ranged from 2.45 to 2.27

Cirrus Data

December 1

S/C ephemeris data were not available so that analysis of this day's spectra were not performed

December 2

$\tau = .780 \pm .065$ $\qquad\qquad$ $R = 3.208 \pm .371$

The air mass ranged from 3.62 to 3.46

$\tau = .780 \pm .064$ $\qquad\qquad$ $R = 3.238 \pm .498$

The air mass ranged from 3.46 to 3.37

January 18

$\tau = .454 \pm ..089$ $R = 3.173 \pm .841$

The air mass ranged from 3.84 to 3.82

Frontal Clouds

August 5

Not analyzed

August 9

$\tau = .515 \pm .150$ $R = 3.111 \pm .661$

...he air mass ranged from 3.16 to 2.94

January 25

$\tau = .632 \pm .053$ $R = 3.435 \pm .641$

The air mass ranged from 2.86 to 2.78

$\tau = .625 \pm .062$ $R = 3.297 \pm .549$

The air mass ranged from 2.78 to 2.71

$\tau = .525 \pm .123$ $R = 3.105 \pm .876$

The air mass ranged from 2.70 to 2.65

III.   Scattering Calculations and Cloud Models

A.   Cloud Models

Both water and ice clouds were assumed to have Gaussian particle size distributions. For the liquid water clouds particles sizes of 1-20 μm were assumed, with 1 and 20 μm being cut-off limits. The calculations were performed in increments of 1 μm. Mean radii of 4, 8, 12, and 16 μm were assumed as were standard deviations of 0.5, 1.0, and 2.0 μm. For the ice clouds the particles were represented as equivalent spheres of radii of 10-100 μm in increments of 10 μm. Mean radii of 30, 50, and 70 μm were assumed as were standard deviations of 5, 10, and 15 μm.

B.   Scattering Calculations

The calculations were performed using techniques described in $\begin{bmatrix} 4, & 5 \end{bmatrix}$. The calculations use indices of refraction derived from Irvine and Pollack $\begin{bmatrix} 6 \end{bmatrix}$.

The indices of refraction are used to compute a Mie scattering function for a spherical droplet. The drop size distribution is combined with the single particle scattering function to yield a phase function for single scattering layer. By a layer doubling technique, the scattering properties of thicker layers may be computed. Computations were performed for wavelengths of .76 μm, 1.61 μm, 2.06 μm, and 2.12 μm. The computations included a range of albedoes which can be related to absorption taking place in the cloud layer. The range of values is given in Table 3.

Table 3

Wavelength	.76 µm	1.61 µm	2.06 µm	2.12 µm
Albedo (water)	0.9, 1.0	.95, .975, 1.00	.95, .975, 1.00	.95, .975, 1.00
Albedo (ice)	0.1, 0.2, 0.3, 0.4	.80, .85, .90, .95	.95, .975, 1.00, 0.2, 0.4, 0.6, 0.8	.75, .80, .85, .90

The computations are for ten discrete solar incidence and satellite viewing angles whose cosines range from 0.05 to 0.95 in increments 0.1. This generates a 10 x 10 scattering matrix.

C. Representative Calculations

As the preceding discussion indicates a tremendous number of scattering matrices were computed. It would be prohibitive to reproduce all of these matrices for this report but representative results will be given.

Ratios of the out-of-band channels are also of interest to this investigation. They are: $S(.76)/S(2.12)$, $S(.76)/S(1.61)$, and $S(1.61)/S(2.12)$, S = scattering matrix. The ratio, $S(1.61)/S(2.12)$, was to determine the thermodynamic phase of the cloud particles. As can be seen from Figure 5, theoretically there is an adequate separation, however, experimental data presented in Section V indicate there is not sufficient resolution to reliably differentiate between water and ice clouds. The ratio, $S(.76)/S(1.61)$, is currently considered a better choice to give this information. Results for this ratio are given in Figure 6.
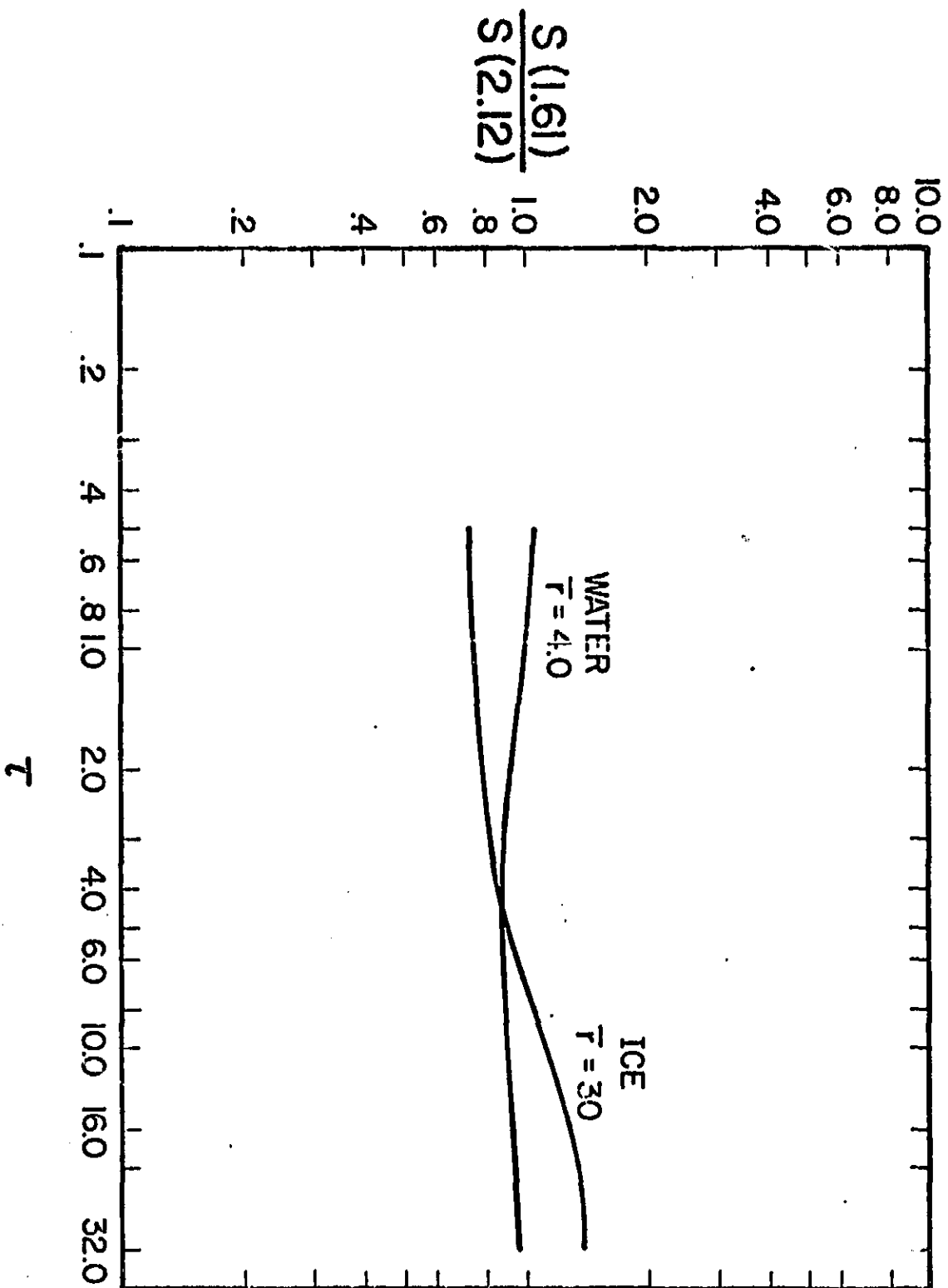
FIGURE 5. THE RATIO, S(1.61)/S(2.12), IS SHOWN AS A FUNCTION OF OPTICAL THICKNESS FOR WATER AND ICE CLOUDS. FOR THE WATER CLOUD, $\bar{r}$ = 4 μm and σ = 0.5 μm. FOR THE ICE CLOUD $\bar{r}$ = 30 μm AND σ = 5 μm.

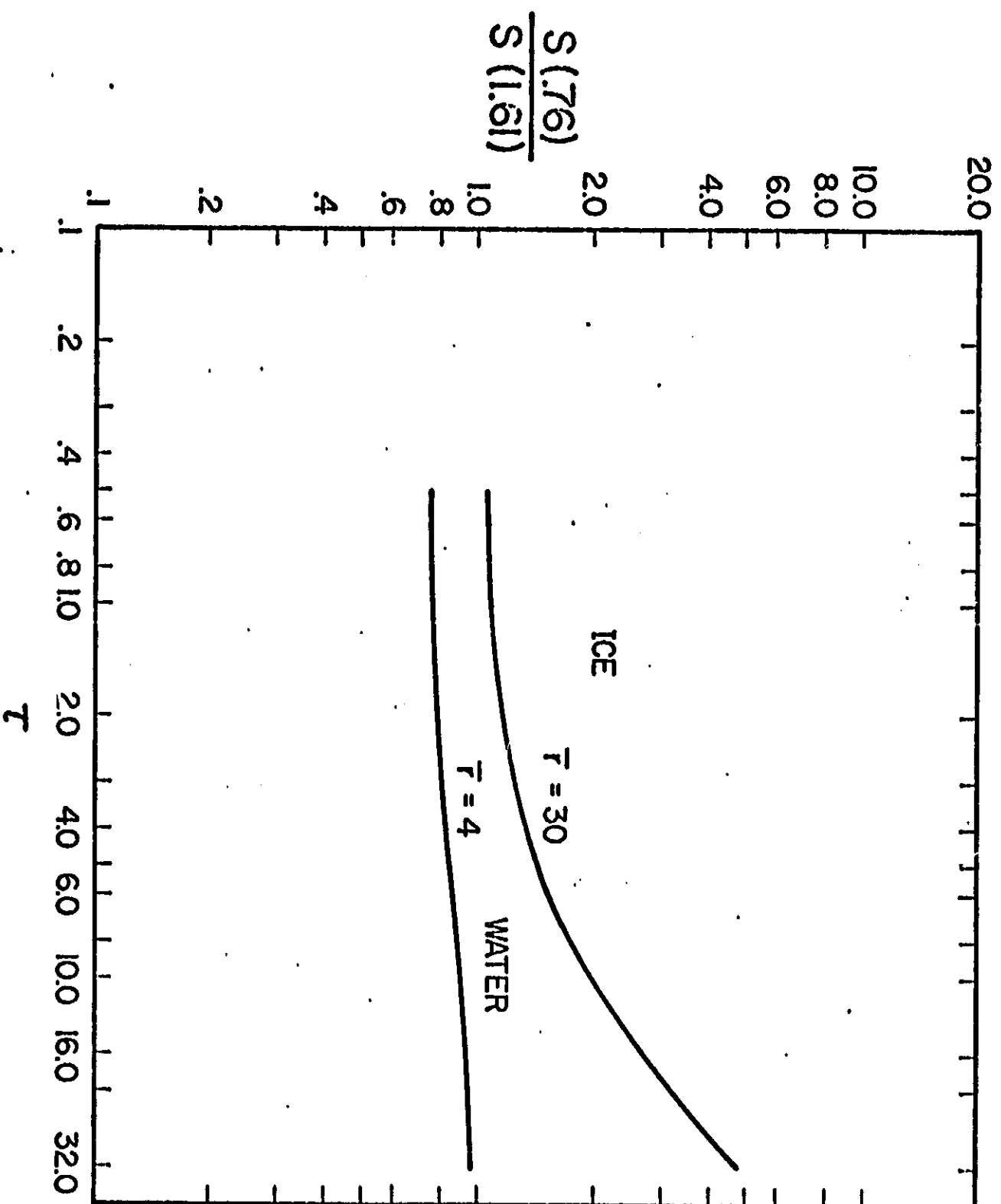FIGURE 6. THE RATIO, S(.76)/S(1.61), IS SHOWN AS A FUNCTION OF OPTICAL THICKNESS FOR WATER AND ICE CLOUDS. THE SIZE DISTRIBUTIONS ARE THE SAME AS IN FIGURE 5.

The particle size parameter is to be inferred from the ratio, S(.76)/S(2.12). Figure 7 a shows results for two size distribution of liquid water drop size distributions and Figure 7 b shows results for two ice cloud distributions.

The computations were carried out for a wide range parameter as indicated in Table 3 and in Sec. III. A. For the water droplet clouds, mean radii of 4 and 16 μm and standard deviations of 0.5 and 2 μm were chosen. These values represent extremes in the size distributions. For the water clouds an albedo of 1 was chosen for all wavelengths. This is the maximum theoretical value as determined from the absorption properties of water.

For ice clouds, mean radii of 30 μm and 70 μm and standard deviations of 5 and 15 μm were used. These values represent extremes in ice cloud models used. For the ice clouds the maximum theoretical albedo also was used for all wavelengths. For .76 μm this albedo value is 1.0; for 1.61 μm it is .95; and for 2.12 μm it is .90. In all cases the calculations are for solar incidence and satellite viewing angles whose cosines are .95 (i.e., 18°).
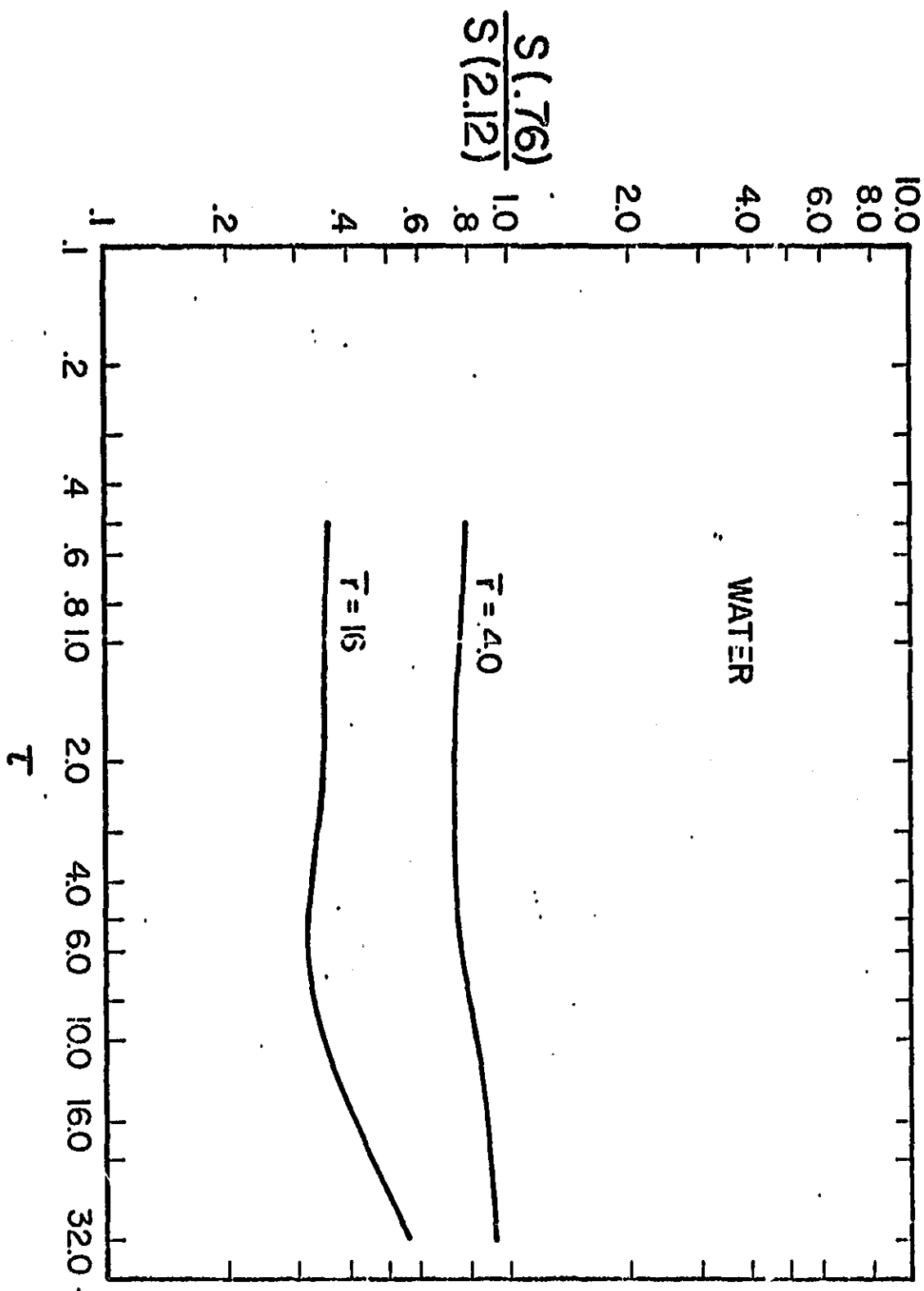
FIGURE 7a. THE RATIO S(.76)/S(2.12) IS SHOWN FOR TWO WATER CLOUDS
AS A FUNCTION OF OPTICAL THICKNESS. THE SIZE DISTRIBUTIONS ARE:
$\bar{\lambda}$ = 4 μm, σ = 0.5 μm AND $\bar{r}$ = 16 μm, σ = 2 μm.
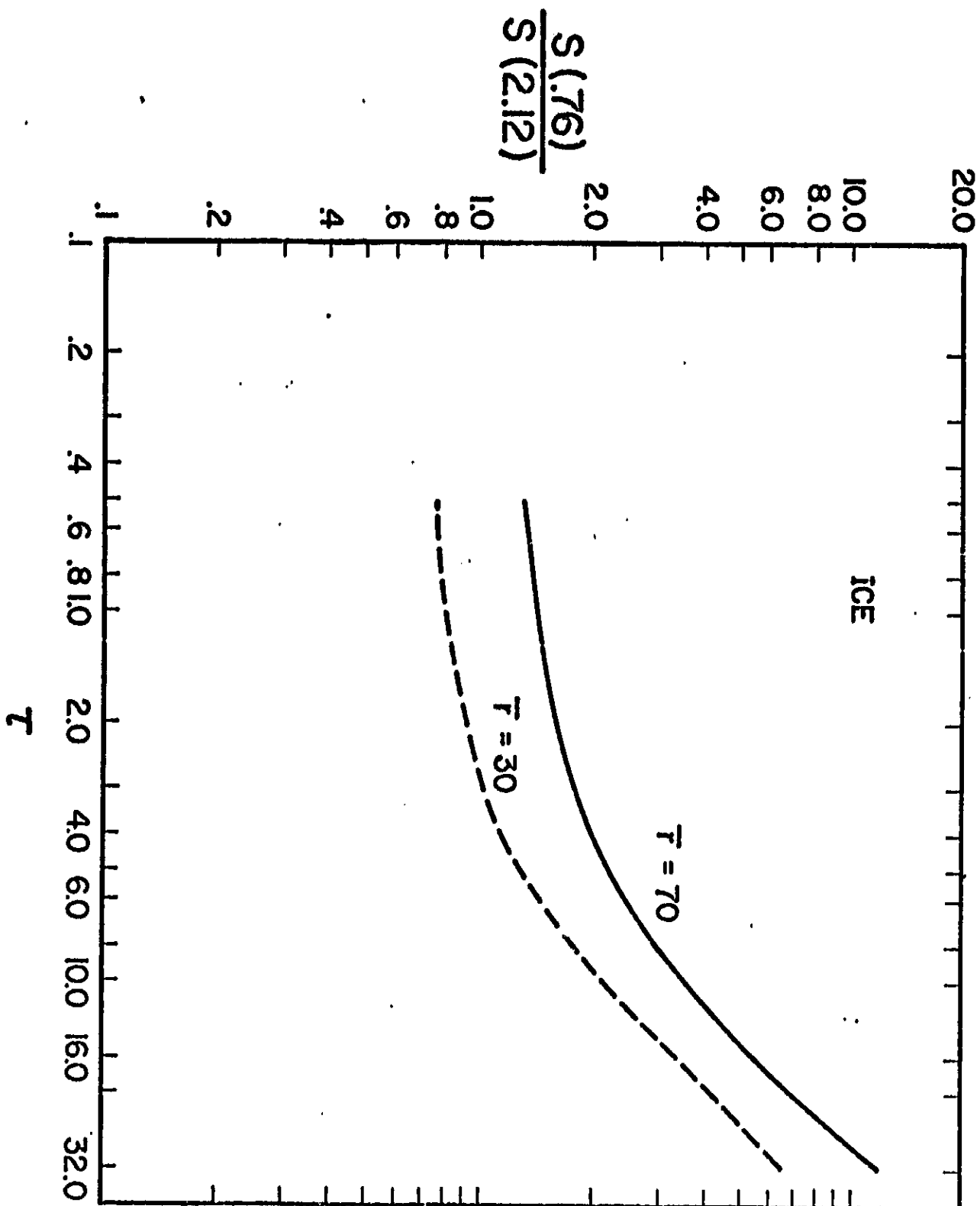
FIGURE 7b. THE RATIO S(.76)/S(2.12) IS SHOWN AS A FUNCTION OF
OPTICAL THICKNESS FOR TWO ICE CLOUDS. THE SIZE DISTRIBUTIONS
ARE: r̄ = 30 µm, σ = 5 µm AND r̄ = 70 µm, σ = 15 µm.

IV   Background Data

A.   Spacecraft Measurements

An important part of any measurements program is an independent
verification of the parameters being observed. For the Cloud Physics
Investigation these verifications came from a variety of sources.
Some verifications were obtained from flights of NASA-JSC aircraft,
other verifications were obtained from pilot reports filed with the
National Weather Service usually by commercial air line pilots,
other sources were radar observations of thunderstorm tops, National
Weather Service weather maps, and topographical maps.

Tables 4 and 5 give the relevant parameters for the SL-3 and
SL-4 data.

Table 4

SKYLAB 3

Date	DOY	Ground Track	EREP Pass	Time (GMT)	Location	Observations
5 Aug.	217	61	14	Not Analyzed	43.96 N, 105.85 W to 46.46 N, 94.19 W	A nadir cross section of frontal clouds associated with a low.
8 Aug.	220	34	16	15:57:21 15:58:50	45.27 N, 125.28 W	An angular scan of off-shore coastal stratus.
9 Aug.	221	47	17	13:43:53– 13:44:55	43.86 N, 91.38 N to 42.03 N, 87.09 W	A nadir cross section of frontal clouds associated with a low.
10 Sept.	253	16	31	20:03:50– 20:05:30	30.22 N, 120.28 W	An angular scan of coastal stratus, NASA P-3 reported bases at 2 kft, tops at 3.5 kft. Unfortunately no DAC.
12 Sept.	255	43	35	Not Analyzed	26.35 N, 91.23 N 31.63 N, 85.23 W	A series of Cb were cited and measured, radiometric data of poor quality.
15 Sept.	258	16	43	18:01:17– 18:03:13	27.35 N, 122.97 W	An angular scan of coastal stratus.

Table 5
SKYLAB 4

Date	DOY	Ground Track	EREP Pass	Time (GMT)	Location	Observations
1 Dec	335	34	55	Not analyzed	37.45 N, 106.9 W to 36.1 N, 104.9 W	Nadir observations of jet stream cirrus. No S/C ephemeris data.
2 Dec	336	48	56	16:43:43-16:44:26	40.2 N, 82.8 W to 35.0 N, 99.3 W	Ci canopy associated with a cold front.
11 Jan	011	58	81	17:34:27-17:35:04	39.1 N, 94.0 W	An angular scan of a snow field Sfc P = 1027 mb, elevation = 0.2 - 0.. km.
12 Jan	012	1	82	16:51:55-16:52:19	around 38.9 N 90.4 W	An angular scan of two snow covered areas near St. Louis, Mo. Sfc P = 1039.4 mb, elevation = 170 m.
18 Jan	018	19	85	20:36:02-20:36:40	48.3 N, 116.2 W to 47.6 N, 112.8 W	Nadir observations of Ci canopies.
18 Jan	018	19	85	Not analyzed	38.1 N, 90.3 W	Partial angular scan of thin Ci and broken snow cover, pirep indicates tops at >2o kft.
20 Jan	020	47	86	19:09:05-19:10:05	near 50.5 N 111.8 W	Angular scan of snow field. Sfc P = 1020 mb, elevation = 0.5 - 1.0 km.

Date	DOY	Ground Track	EREP Pass	Time (GMT)	Location	Observations
22 Jan	022	5	88	19:20:34-19:22:06	near 42.9 N 107.4 W	Sfc P = 1024 mb, elevation = 1-2 km, angular scan of snow field.
24 Jan	024	33	89	17:55:31-17:56:02	near 47.3 N 101.7 W	Sfc P = 1022 mb, elevation = 0.5 - 1 km, angular scan of snow area.
24 Jan	024	33	89	17:56:46-17:57:03	near 42.3 N 92.6 W	Angular scan of snow area Sfc P = 1024 km, el = 0.2-0.5 km.
25 Jan	025	47	90	17:17:26-17:19:28	38.85 N, 80.9 W to 31.4 N, 70.1 W	Nadir observations of frontal clouds, pirep indicates tops >37 kft, NASA aircraft flew from 37 N 78 W to 39 N, 81.5 W reported tops 30-40 kft, Hasselblad pictures taken.
31 Jan	031	62	97	Not analyzed	about 88 W, 31 N to 86 W, 29 N	Frontal clouds just beyond Mobile. No DAC.

B. Calibration Results

As indicated in Section II significant difficulties were encountered with the wavelength calibration in the A band region of the spectrum. Our initial treatment of the problem was based on data given on p. 3.7-7 of [7]. This approach was to fit a series of three straight lines of the form $\lambda = A_o + A_1 V$ to region between .681 μm and .878 μm. Segment 1 was between .681 and .745 μm; Segment 2 was between .745 and .753 μm and Segment 3 was between .753 and .878 μm. Subsequently it was learned that most of the data given in the table on p. 3.7-7 in [7] was interpolated and apparently used a quadratic interpolation formula. The results of this approach resulted in the center of A band being shifted to shorter wavelengths by amounts of .01 μm or greater. Since the A band has been extensively studied in the laboratory and its center is known very accurately, it was decided to use the A band as a calibration point. Figure 8 shows a plot of ramp voltage vs wavelength for the three Schott glass absorption bands and the oxygen A band. A least squares straight line was fit to the two longer wavelength Schott glass bands and the center of the A band. The equation for this interval, given in [8], is also linear and therefore easily inverted. This equation was used between .672 and .744 μm. The least squares equation was used between .745 μm and .874 μm. More precisely we used

$$\lambda = A_1 C + A_o \text{ for } 740 \leq C \leq 762$$

where λ = wavelength in micrometers

$A_o = -1.7567$.

$A_1 = 3.2819 \times 10^{-3}$
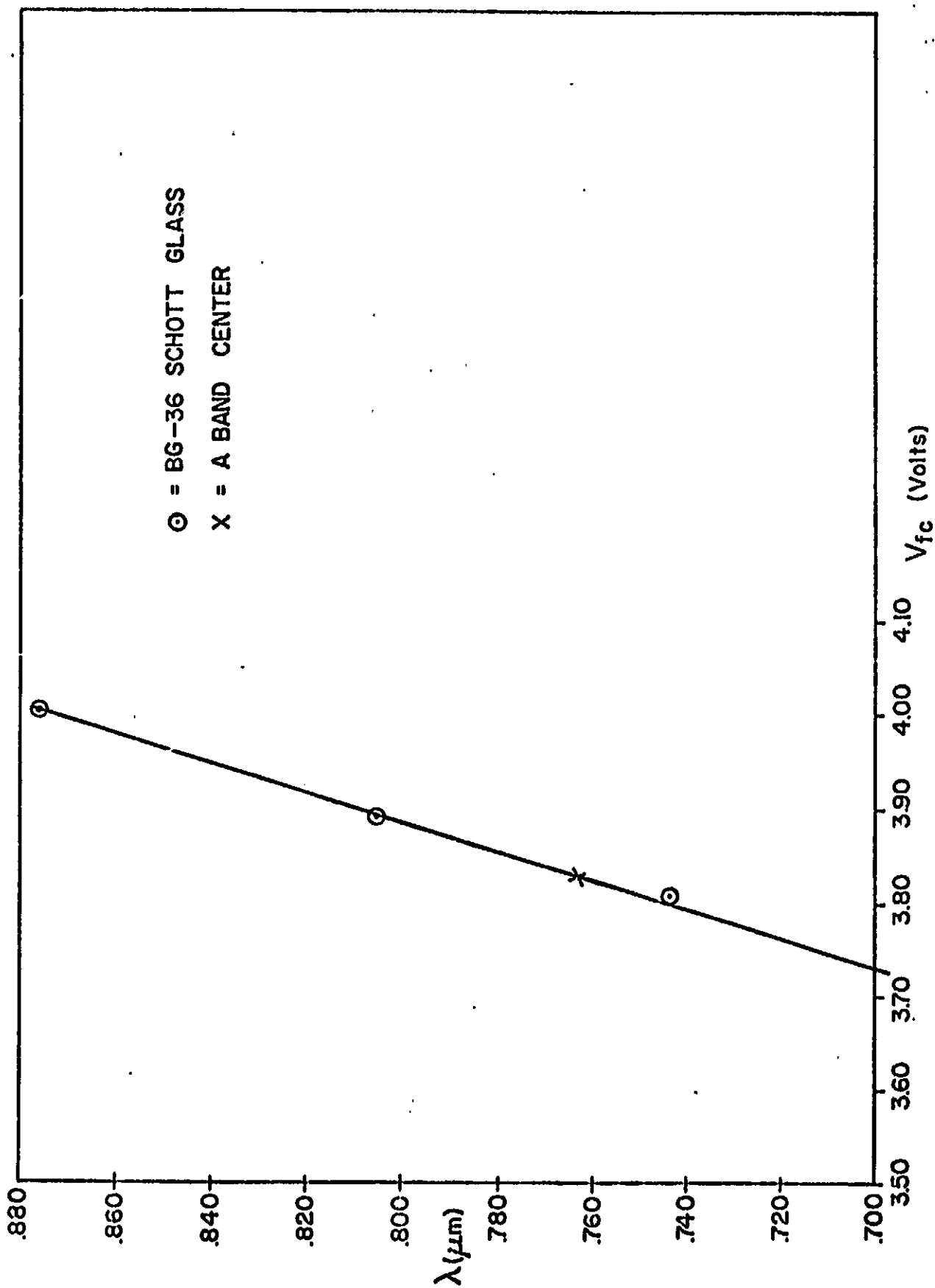
C = no. of counts

FIGURE 8   THIS FIGURE SHOWS WAVELENGTH AS A FUNCTION OF RAMP VOLTAGE.   THE SCHOTT
GLASS VOLTAGES ARE TAKEN FROM SL-3 CALIBRATION DATA.   THE A BAND CENTER VOLTAGE
WAS ALSO DETERMINED FROM DATA TAKEN DURING SL-3.

and for $763 \leq C \leq 800$

$$\lambda = A_1 C + A_o$$

where $A_o = -1.73655$

$$A_1 = 3.263 \times 10^{-3}$$

The equations given in [8] would be of more value to users if they were inverted (i.e., the ramp voltage should be the independent variable rather than the wavelength).

Significant discrepancies were noted between transmittance values calculated using the Lowtran 2 program and those values derived from the S-191 measurements. (Compare values given on pps. 9-11 and Fig. 4.) A number of possibilities have been hypothesized and investigated in an attempt to explain the differences. The wavelength calibration was among the possibilities considered. This was an area of particular concern as no calibration points beyond 1.91 μm were used. Parenthetically it should be noted that there are a number of absorption features in the atmosphere between 2.4 and 2.5 μm which could have been used as calibration points.

Figure 9 illustrates the reason for the concern about wavelength calibration. The curve labeled I_c is an intensity curve computed from the transmission spectra from Lowtran 2, a triangular instrument response function of half-width .03 μm, and solar irradiance spectra. This curve has been normalized to 2.125 μm. The atmosphere is a tropical model. The curve labeled τ_c is the transmission spectra computed from Lowtran 2. Its spectral resolution is .008 μm. The

curve labeled I_m is a measured spectrum of coastal stratus taken September 10. It also has been normalized to 2.125 μm. The shapes of the spectra seem to suggest that the S-191 spectra are offset by between .01 and .02 μm to the short wavelength side. The S-191 spectra also seem to show an anomalously steep and long rise after the absorption minimum at 2.06 μm.
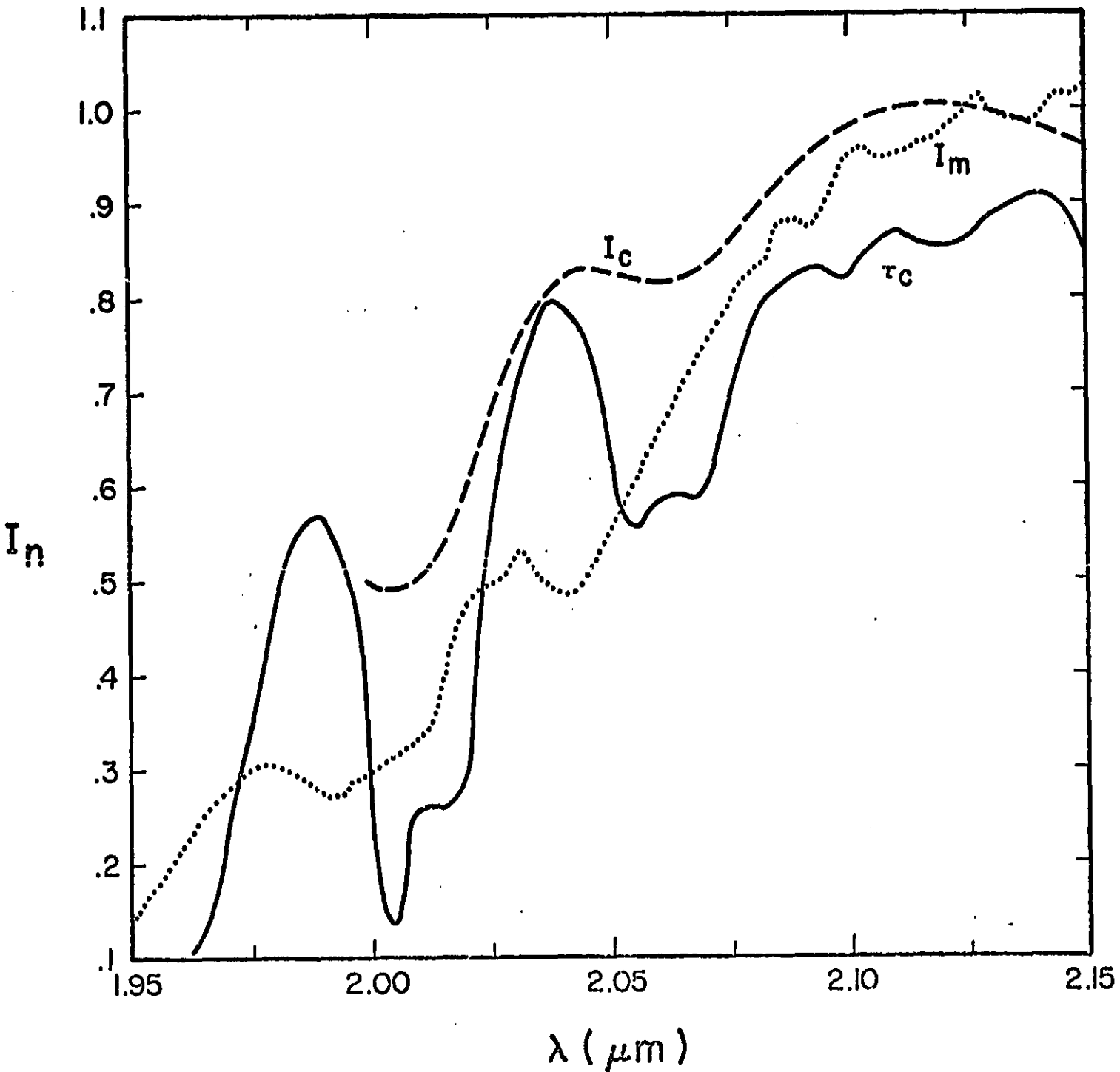
FIGURE 9   THIS FIGURE SHOWS NORMALIZED INTENSITY AS A FUNCTION OF WAVELENGTH.
I_C IS A CALCULATED AND NORMALIZED VALUE. I_M IS A MEASURED VALUE THAT HAS ALSO
BEEN NORMALIZED. τ_C IS A CALCULATED ATMOSPHERIC TRANSMISSION.   ITS SPECTRAL
RESOLUTION IS .008 µM.   THE INTENSITIES HAVE .03 µM SPECTRAL RESOLUTION.

V. Data Analysis

The first impressions of the snow data are somewhat disturbing. One notes that the measured transmittances are significantly lower than those predicted in Figure 4. In some cases this difference is a factor of two. The other point is the large standard deviations encountered. These are typically 20% and greater. While somewhat disappointing in themselves, nevertheless explanations of some type are possible.

Several possible explanations for the anomalously low transmission values were investigated and some were discussed in Section IV. The best explanation however is that snow has a difference in absorption between 2.06 μm and 2.125 μm. This difference can be quite significant for some kinds of snow [9].

The reflectivity of snow is quite high in the visible but decreases rapidly for wavelengths greater than 1.0 μm, reaching a minimum at about 2 μm. Thus the instrument had a very poor signal to noise ratio for these wavelengths and hence the large variations in transmission observed.

This decrease in reflectance can be exploited however. Based on the analysis of only a few days data, it appears to be possible to differentiate between snow cover and clouds simply by taking the ratio I(.754)/I(2.125). For example, January 20 (Snow) I(.754)/I(2.125) = 161 ±63 and September 10 (Coastal Stratus) I(.754)/I(2.125) = 26.4 ±1.9. The large uncertainty in the snow ratio is due to the low values of I(2.125).

Originally it was intended that the ratio I(1.61)/I(2.125) would provide discrimination between water and ice clouds and possibly snow cover as well. The data obtained during this investigation tend to show

this is not a viable consideration. The two highest ratios are obtained for the coastal stratus cases of August 8 and September 10, which most probably are liquid water droplets. The coastal stratus values of September 15 however fall into the range of cirrus cloud ratios. The frontal clouds show a range of values and rather wide standard deviations. Similarly there is considerable overlap between the cirrus ratios and the snow ratios. The snow ratios tend to be higher but possess large standard deviations.

VI. Summary and Conclusions

Further analysis of the short wavelength (i.e., the oxygen A band) data is continuing but it appears unlikely that it will be completed in time for inclusion in this report.

This investigation has produced a number of positive results. As a result of this program a number of new scattering calculations for various models have been performed. An atmospheric transmittance program to calculate transmittances on a line-by-line basis was developed for the oxygen A band. A copy of the Lowtran 2 program was obtained and modified slightly for this investigation's particular requirements. Thus a comprehensive set of theoretical "tools" have been acquired and can be used to assess the problem.

Useful insights into spectral resolution requirements, wavelength calibration, accuracy and dynamic range needs have been gained during this investigation. A number of these insights have been gained in the process of analyzing the S191 data.

The determination of five parameters associated with clouds was the goal of this experiment. These parameters are: (1) cloud top pressure altitude, (2) thermodynamic phase, (3) optical thickness, (4) a particle size parameter, and (5) particle density. Cloud top pressure altitude   This parameter was our single most important coal. No cloud top pressure altitudes were inferred from the S-191 data. The most important reason for this is that no A band transmittances were obtained. Due to the wide spectral resolution

and variable wavelength sampling no transmittances in the A band region were deduced. This is discussed more fully in Sec. II. B. 2. Transmittances which were anomoulously low were deduced in the 2.0 μm CO_2 absorption band. There are also wavelength calibration uncertainties in this region.

Thermodynamic phase   Originally the ratio of $I(1.61)/I(2.125)$ was to be used to determine the thermodynamic phase. Sufficient results were obtained from snow, cirrus, and coastal stratus to indicate this ratio is probably not a reliable indicator of snow, ice particles or water droplets.

Optical thickness   The technique to be used for this was dependent on an absolute determination of cloud reflectance at .754 μm. The spectral resolution at .754 μm was such that it overlapped into a water vapor band and the A band itself. These difficulties coupled with the wavelength calibration uncertainties and program time constraints were such that no attempts to infer optical thickness were made. No "in situ" measurements of optical thickness were made, and estimates from geometrical thickness would be extremely crude.

Particle size   No attempt was made to infer a particle size parameter. As can be noted in Figs. 7a and 7b an estimate of the optical thickness is required to make a particle size determination. This estimate was not available. Also no "in situ" measurements of particle size were available.

Particle density   This is probably the most difficult determination of the five, depending in particular on optical thickness and particle size. No attempts were made to determine particle density and no "cloud truth" of this parameter was available.

References

1. Burch, D. E. and D. A. Gryvnak, "Strengths, Widths, and Shapes of the Oxygen Lines Near 7600 Angstroms", Report U-4076 Philco-Ford Corp., Aeronutronics Division, Newport Beach, California, May, 1967.

2. Selby, J. E. A. and R. M. McClatchey, "Atmospheric Transmittance From 0.25 to 28.5 um: Computer Code LOWTRAN 2 Environmental Research Paper No. 427, AFCRL, Hanscom Field, Bedford, Massachusetts, December 1972.

3. Thekaekara, M. P., "Solar Electromagnetic Radiation" NASA SP-8005, NASA-GSFC, Greenbelt, Maryland, May, 1971.

4. Twomey, S., H. Jacobowitz, and H. B. Howell, Matrix Methods for Multiple-Scattering Problems", J. Atmos. Sci., 23, 289, 1966.

5. Twomey, S., H. Jacobowitz, and H. B. Howell, "Light Scattering by Cloud Layers", J. Atmos. Sci., 24, 70, 1967.

6. Irvine, W. M., and J. B. Pollack, "Infrared Optical Properties of Water and Ice Spheres", Icarus, 8, 324, 1968.

7. "Earth Resources Experiment Package--Experiment Calibration Data", Document No. MSC-07744, Lyndon B. Johnson Space Center, Houston, Texas, January 1973.

8. "Earth Resources Experiment Package--Sensor Performance Evaluation" Final Report, Vol. II (S191), Document No. MSC 05546, Lyndon B. Johnson Space Center, Houston, Texas, January, 1975.

9. O'Brien, H. W. and R. H. Munis, "Red and Near-Infrared Spectral Reflectance of Snow" Research Report 332, U. S. Army, Cold Regions Research and Engineering Laboratory (CRREL) Hanover, New Hampshire, March, 1975.